NONLINEAR ANALYSIS OF REINFORCED CONCRETE FRAMES CONSIDERING THE STRAIN-SOFTENING OF CONCRETE

변형연화현상을 고려한 철근콘크리트 골조의 비선형 해석

김 진 근* 이 태 규**
Kim, Jin-Keun Lee, Tae-Gyu

요 약

휨을 받는 철근콘크리트 부재 단면의 연화현상은 구조물의 파괴하중 해석시 중요한 인자로 작용한다. 일반적인 탄-소성 이론에 근거한 소성한계해석법을 사용할 경우 철골 구조물에는 적합하지만 철근콘크리트 구조물에는 최대하중 이후의 연화현상으로 인하여 이 이론은 부적합하게 된다. 따라서 본 논문의 주목적은 변위제어방법을 사용하여 철근콘크리트 구조물이 파괴될 때까지의 완전한 거동을 이끌어 내는 것이다.

프로그램을 사용한 계산결과를 보다 빠르고 경제적으로 이끌어 내기 위하여 단면의 성질인 모멘트-곡률, 축력-축방향 변형률, 그리고 전단력-전단 변형률 곡선 등을 여러 개의 직선식으로 단순화한 모델식을 사용하여 해석한다. 또한 연화현상을 고려한 유한요소의 해석결과는 사용된 요소의 크기에 따라 결과가 매우 다르게 나타나기 때문에 이를 방지하기 위하여 파괴에너지 개념을 도입하여 모멘트-곡률 곡선을 보정하여 구조계산에 적용시킨다. 이와 같이 단면을 층으로 나누어 해석하지 않고 직접 단면의 성질을 나타내는 곡선들을 적용한 본 프로그램으로 보와 골조를 해석한 결과는 실제적인 실험결과와 비교하였을 경우 거의 일치하게 나타난다.

ABSTRACT

Softening of reinforced concrete sections at advanced curvatures in flexure is taken into account in collapse load analysis of frames. The entire load-deflection relation for cracking reinforced concrete frame is analyzed by displacement control method. For further simplification, the linearized forms of section behavior for combined flexure, shear and axial force are used. The result of analysis by finite element method for the materials with strain-softening is shown to spurious sensitivity to the chosen finite element size. If the moment-curvature curve is modified for each element by introducing the conecpt of fracture energy approach, this problem can be overcome. It is shown that this analytical result predicts well the experimental result for softening structure.

* 정회원, 한국과학기술원 토목공학과 부교수, 공학박사
** 준회원, 한국과학기술원 토목공학과, 박사과정

● 1989. 9. 9 접수. 본 논문에 대한 토론을 1990. 3. 31까지 본 학회에 보내주시면 1990. 6월호에 그 결과를 게재해 드리겠읍니다.

1. INTRODUCTION

Plastic limit analysis, which is commonly used, quite differs from steel and concrete frame structure. For steel frames, a collapse load analysis based on the assumption of elastic-perfectly plastic theory provides the basis for the plastic limit analysis. The extensive ductility of typical steel sections at plastic state provides realism to the basic assumption and the existence of a strain-hardening range provides a factor of safety. When loaded to destruction, however, reinforced concrete frames exhibit a softening response in which the load, after reaching its peak value, does not follow a constant-load yield plateau but gradually declines at increasing displacement because of the limited ductility and strain-softening behavior of typical concrete sections. Due to the absence of yield plateau, the conditions of plastic limit analysis are not satisfied.

For this reason, we attempt here to analyze the problem by the displacement control method, which makes it possible to follow the response up to the snapback point, if such a point exists. This paper deals with collapse load analysis of frames, based on an assumption of behavior of sections subjected to combined flexure, shear and axial force to be performed. The purpose is to obtain the entire load-deflection curve for strain-softening structures in order to determine the collapse load and the postpeak behavior, and thereby to provide a speedy, realistic, and economical method for the assessment of collapse loads.

2. CONSTITUTIVE LAWS OF CONCRETE AND REINFORCING BAR

In this study, the stress-strain curve of reinforcing bar in tension and compression is assumed to be elastic-perfectly plastic. For concrete in compression, the stress-strain curve is assumed as the following expression and is shown in Fig. 1. The tensile strength of concrete is neglected.

$$\sigma_c = \frac{f_c'}{\epsilon_p} \mathrm{Exp}\left\{ \frac{1}{m} \left[1 - \left(\frac{\epsilon_c}{\epsilon_p} \right)^m \right] \right\} \epsilon_c \quad (1)$$

$$\epsilon_p = 1.49 \times 10^{-5} f_c' + 0.00195 \quad [2] \quad (2)$$

where, ϵ_c : strain of concrete

ϵ_p : strain of concrete at ultimate compressive strength

σ_c : stress of concrete corresponding to strain ϵ_c, MPa

f_c' : ultimate compressive strength of concrete, MPa

m : empirical constant

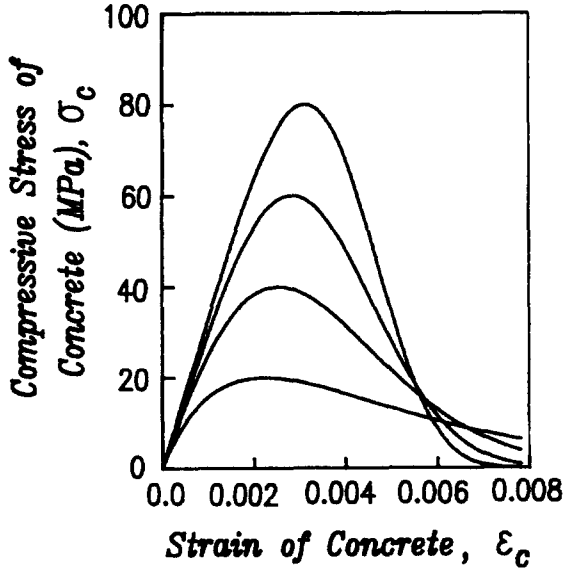

Fig. 1 Stress-Strain Curve of Concrete in Compression

Using $E_c = 9.11\times10^3\ f_c'^{0.3}$(MPa)for Young's modulus of concrete[3], we may evaluate the constant as Eq. 3.

$$ln\left(9.11\times10^3\frac{\epsilon_p}{f_c'^{0.7}}\right)=\frac{1}{m}\left[1-\left(\frac{f_c'^{0.7}}{2.28\times10^4\epsilon_p}\right)^m\right] \quad (3)$$

But the constant m is evaluated from the proposed second order equation as Eq. 4 because it is impossible to find the constant m directly. The comparison between Eq. 3 and Eq. 4 is shown in Fig. 2.

$$m = 0.3574+2.55\times10^{-2}f_c'+2.25\times10^{-4}f_c'^2 \quad (4)$$

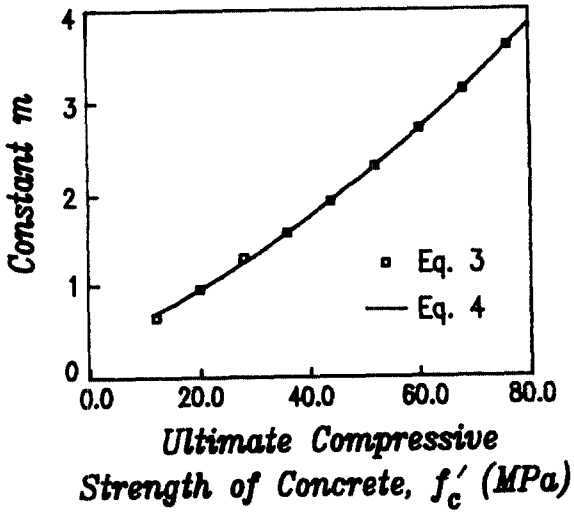

Fig. 2 Relation of Compressive Strength of Concrete and Constant m

3. NONLINEAR ANALYSIS METHOD

3.1 Conversion into the Displacement Control

In this paper, we convert the load control method into the displacement control method in nonlinear analysis. The load control method is that the applied load vector {f} is given, then the unknown displacement vector {u} can be solved by the iteration scheme. In the displacement control method, meanwhile, if the p-th displacement u_p is controlled as known value, the applied load vector {f} and displacements which are not controlled are unknowns. Since each load which acts on a structure can be expressed in terms of a certain load f_j, the total load vector {f} can be written as Eq. 5. Finally, we obtain the resultant simultaneous equation of Eq. 6.

$$\begin{Bmatrix} f_1 \\ f_2 \\ \vdots \\ f_j \\ \vdots \\ f_n \end{Bmatrix} = \begin{Bmatrix} m_1 \\ m_2 \\ \vdots \\ m_j \\ \vdots \\ m_n \end{Bmatrix} \{f_j\} \quad (5)$$

where, $m_1, m_2, \cdots, m_j, \cdots, m_n$: constants

$$\begin{bmatrix} K_{11} & K_{12} & \cdots & -m_1 & \cdots & K_{1n} \\ K_{21} & K_{22} & \cdots & -m_2 & \cdots & K_{2n} \\ \vdots & \vdots & & \vdots & & \vdots \\ K_{p1} & K_{p2} & \cdots & -m_p & \cdots & K_{pn} \\ \vdots & \vdots & & \vdots & & \vdots \\ K_{n1} & K_{n2} & \cdots & -m_n & \cdots & K_{nn} \end{bmatrix} \begin{Bmatrix} u_1 \\ u_2 \\ \vdots \\ f_j \\ \vdots \\ u_n \end{Bmatrix} = \begin{Bmatrix} -K_{1p} \\ -K_{2p} \\ \vdots \\ -K_{np} \\ \vdots \\ -K_{pp} \end{Bmatrix} u_p \quad (6)$$

Consequently the unknown loads and displacements in these simultaneous equations can be calculated by iteration until the residual forces converge to the prescribed tolerances and the element stiffness K_{ij}'s are obtained by the Timoshenko beam theory[4].

3.2 Overall Program Structure

A load-deflection curve at a certain point of a structure can be obtained by increasing the displacement of that point and by iteration scheme, as discussed previously, at each increment stage with including the effect of the strain-softening for concrete. To reduce computation time, the stiffness is recalculated only for the first iteration of every increment and kept constant thereafter until convergence of solution is achieved. Fig. 3 shows the overall program structure.

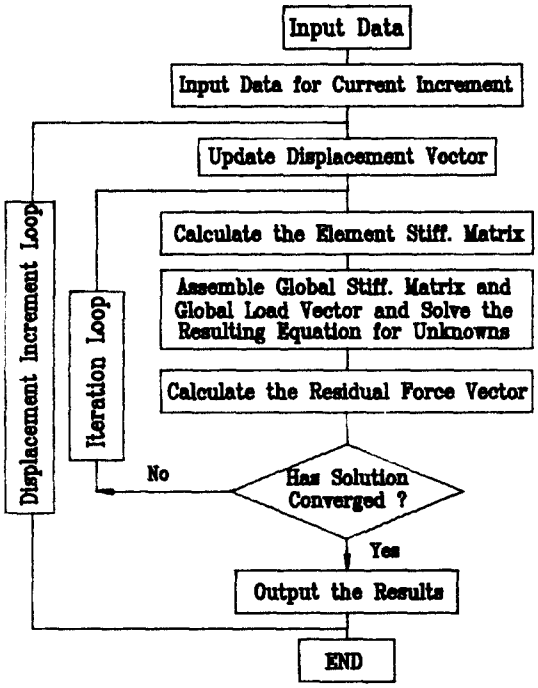

Fig. 3 Overall Program Structure

4. MODELING OF SECTION BEHAVIOR FOR STRUCTURAL ANALYSIS

4.1 Modeling of Moment-Curvature

In a frame, the moment-curvature curve of a given member section should be determined by considering the combined effect of moment and axial force. Based on the curves of two cases pure bending($P=0$) and balanced state($P=P_b$) – the points of maximum moment for each applied axial force are approximately located on a chain line shown in Fig. 4. The following equations are assumed from the relationship of moment-axial force.

At a compressive failure part, that is, the axial force P is greater than P_b ;

$$\left(\frac{P-P_b}{P_o-P_b}\right)+\left(\frac{M}{M_b}\right)^{\alpha}-1 \qquad (7)$$

At a tensile failure part, that is, the axial force P is less than P_b ;

$$\left(\frac{P_b-P}{P_b}\right)+\left(\frac{M-M_o}{M_b-M_o}\right)^{\beta}=1 \qquad (8)$$

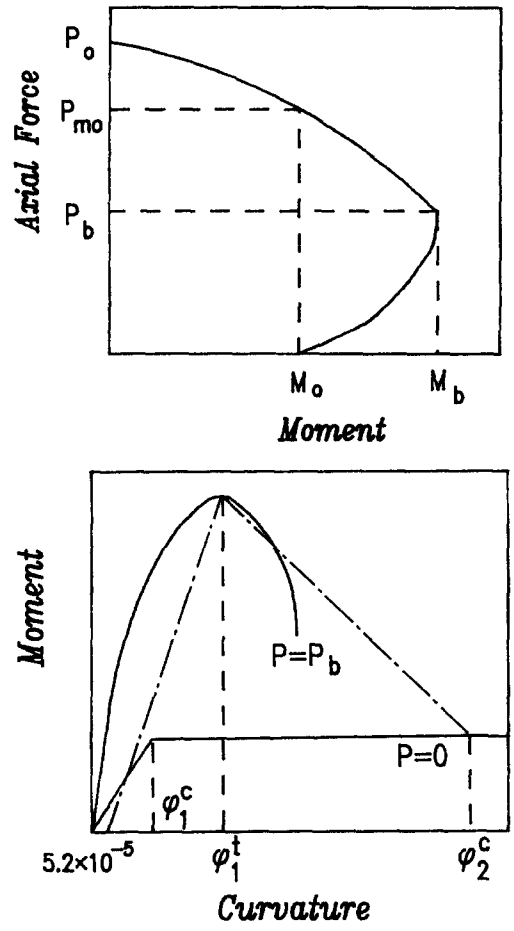

Fig. 4 Location of Maximum Moment and Relationship of Moment-Axial force

where, P_b : balanced axial force, kN

M_b : balanced bending moment, kN-m

P_o : pure axial force, kN

M_o : pure bending moment, kN-m

P_{mo} : axial force when bending moment reaches M_o, kN

α : constant = 1.81 – 0.69A

β : constant = 3.73 – 3.13B

for which P is given value

$$A = \frac{P - P_b}{P_o - P_b}, \quad B = \frac{P_b - P}{P_b}$$

for which M is given value

$$A = \frac{M_b - M}{M_b}, \quad B = \frac{M - M_o}{M_b - M_o}$$

For further simplification, the linearized forms of moment-curvature curves such as so called elastic-softening model and elastic-plastic-softening model for compressive and tensile failure part respectively are used. Fig. 5 shows the linearized relationship expressed in Eq. 9.

$$M_y = (0.975 - 0.005P/P_b) \times M_u$$
$$\phi_1 = \phi_1^t + (\phi_1^c - \phi_1^t) \times P/P_b \qquad (9)$$
$$\phi_2 = 2\phi_2^t - \phi_1$$

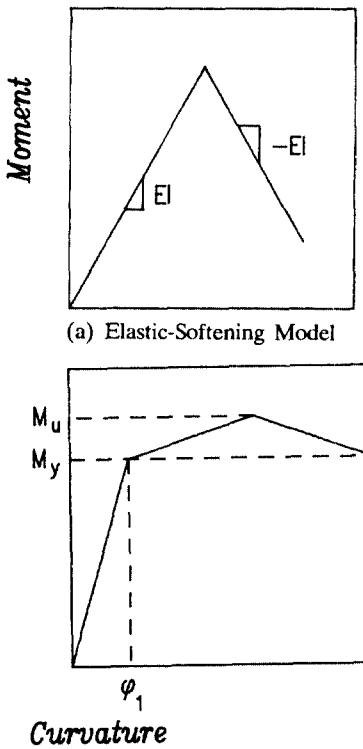

(a) Elastic-Softening Model

(b) Elastic-Plastic-Softening Model

Fig. 5 Simplified Moment-Curvature Relations

4.2 Modification of Moment-Curvature Curve

In concrete structures which show strain-softening, the curvature distribution of a member section indicates a nonlinear form where the bending moment exceeds the yield moment M_y of the section[5] as shown in Fig. 6. The actual curvature distribution at ultimate can be idealized into elastic and inelastic regions as shown in Fig. 6(c).

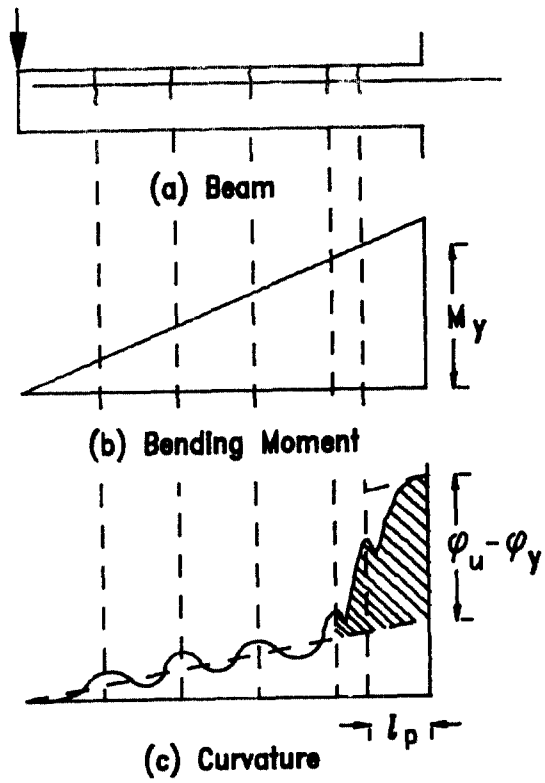

Fig. 6 Curvature Distribution

The shaded area represents the plastic rotation that occurs in addition to the elastic rotation at the ultimate stage of the member. Since the fracture energy for the member to collapse must be constant, the plastic hinge rotation should also have a constant value

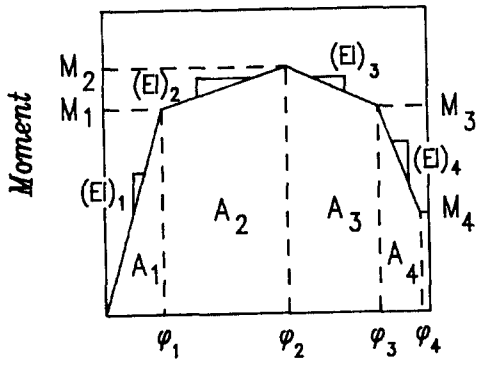

(a) Standard Moment-Curvature Curve

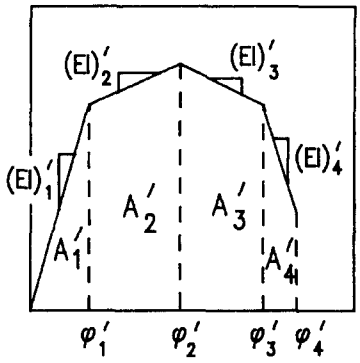

Curvature

(b) Modified Moment-Curvature Curve

Fig. 7 Standard and Modified Moment-Curvature Curves

and should be independent of the chosen element size in the finite element analysis. Therefore, if different element sizes are used in analysis, moment-curvature curves need to be modified in order to obtain consistent results, and it can be achieved by using the fracture energy concept[6].

Fig. 7 shows the standard and the modified moment-curvature curves that mean the moment-curvature curve for the element with the same element length of the plastic length l_p and for other element sizes, respectively. If the chosen element length is l, the area A_i should be equal to the area A_i' which represents elastic zone. The area of inelastic range, however, should be modified as $A_i\, l_p = A_i'\, l$ (i=2, 3, 4). Therefore, the modified slope and curvature[1] can be written as

$$(EI)_i' = (EI)_i \frac{l}{l_p} \tag{10}$$

$$\phi_i' = \frac{l_p}{l}(\phi_i - \phi_{i-1}) + \phi_{i-1}' \tag{11}$$

There are several equations in the literature for the plastic length of flexural beam. For this study the mean value of following two equations – Corley[7] and Mattock[8] – is taken as the plastic length.

$$l_p = 0.5d + 0.32z/\sqrt{d} \tag{12}$$

$$l_p = 0.5d + 0.05z \tag{13}$$

where, d : effective depth of member, cm
z : distance of critical section to the point of contraflexure, cm

4.3 Modeling of Axial Force-Axial Strain

Alike the moment-curvature curve for a given applied axial force, the axial force-axial strain curve also varies continuously according to the applied moment. Accordingly, the

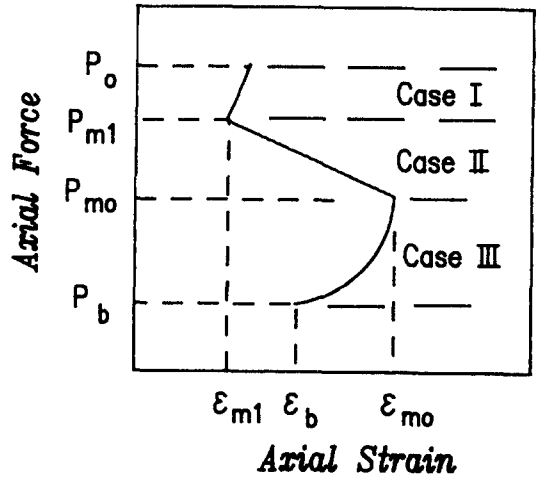

Fig. 8 Location of Maximum Axial Force

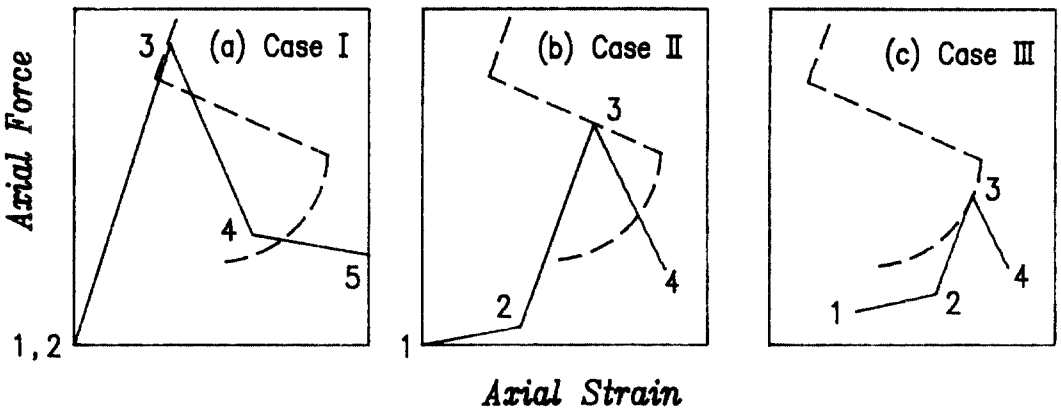

Fig. 9 Linearized Forms for Each Case

Table 1 Positions Assumed for Each Case

		Case I	Case II	Case III
1	P_1	0.0	0.0	$P_b(1-\xi)$
	ε_1	0.0	0.0	$\varepsilon_b(1-\xi)$
2	P_2	0.00	$0.014P_o$	$P_b(1-\xi)+0.014\xi P_o$
	ε_2	0.00	$\varepsilon_a+\left(\frac{\varepsilon_{op}-\varepsilon_a}{P_{m1}-P_{mo}}\right)(P_{m1}-P_m)$	$\varepsilon_b-\xi(\varepsilon_b-\varepsilon_{op})$
3	P_3	P_m	P_m	P_m
	ε_3	$0.53\,\varepsilon_p\left[\frac{P_m}{P_o}+0.887\right]$	$\varepsilon_{m1}+\left(\frac{P_{m1}-P_m}{P_{m1}-P_{mo}}\right)(\varepsilon_{mo}-\varepsilon_{m1})$	$(2.48x^3-3.9x^2+2.43x)\varepsilon_p$
4	P_4	$P_m-(\varepsilon_3-\varepsilon_2)EA_2$	$0.4P_m$	$0.4P_m$
	ε_4	$\frac{P_m-P_g+450P_o\varepsilon_g-EA_2\varepsilon_2}{450P_o-EA_2}$	$\varepsilon_3-\frac{0.6P_m}{EA_2}$	$\varepsilon_3-\frac{0.6P_m}{EA_2}$
5	P_5	$0.85P_3$	———	———
	ε_5	0.01		

$$\xi=\frac{P_m-P_b}{P_{mo}-P_o},\quad x=\frac{P_m-P_b}{P_o-P_b},\quad \varepsilon_a=0.014\varepsilon_{m1}\frac{P_o}{P_{m1}}$$

P_m : maximum axial force for a given moment

ε_{op} : axial strain at which moment reaches M_o

P_g, ε_g : axial force and strain on the second contraflexure point for case I

EA_2 : second axial rigidity for case I

axial force-axial strain curve must be evaluated. The axial force is applied at the plastic centroid of the section, and the axial strain measures at that point.

Fig. 8 shows the location of the maximum axial force for each applied moment, and three different linearized cases of the section behavior is shown in Fig. 9 (see Table 1 for details). Based on the axial force-axial strain relationships of twelve test sections, the parameters of Table 1 are determined by using the statistical method. Case I means the uncracked section behavior. Case II and III means the cracked behavior. That is, a relatively low axial rigidity is noticed when the applied moment is greater than the cracking moment $0.3M_o$[9].

4.4 Modeling of Shear Force-Shear Strain

The basic assumption is that the shear force -shear strain curve varies according to the axial force except combined moment. The relation of axial force-shear force[10] are shown in Fig. 10 and the equation assumed is written by Eq. 14.

$$Q_m = \frac{1.1\times10^{-5}\ f_c'\ A}{0.01+0.68\gamma_m^{1.53}}\ (kN) \qquad (14)$$

$$Q = Q_m\left[1-\left(\frac{P-P_q}{P_o-P_q}\right)^{1.15}\right]\ (kN)$$

$$\gamma_m = 7.44\times10^{-4}+\sqrt{4.61\times10^{-4}f_c'-5.68\times10^{-7}}$$

where, A : area of section, m^2

Q : shear force, kN

P_q : given axial force($=0.5f_c'A$)[10], kN

Q_m : maximum shear force at axial force P_q, kN

γ_m : shear strain corresponding to shear force Q_m

Fig. 11 shows the linearized form of the shear force-shear strain expressed in Eq. 15.

$$\gamma_p = \gamma_m\ Q/Q_m \qquad \text{for } P \quad P_q$$

$$= 0.5\gamma_m(Q-Q_o)/(Q_m-Q_o) \qquad \text{for } P \quad P_q \qquad (15)$$

$$GA_2 = -0.068\ GA_1$$

where, γ_p : shear strain corresponding to shear force Q

Q_o : pure shear force, kN

5. DISCUSSIONS FOR TEST RESULTS

Comparisons are made for two cases ; firstly, results obtained for various element sizes of a under-reinforced beam in the analyses are compared to each other, and compared with experimental test result[11] of which test was subjected to flexural failure, secondly, our analytical result is compared

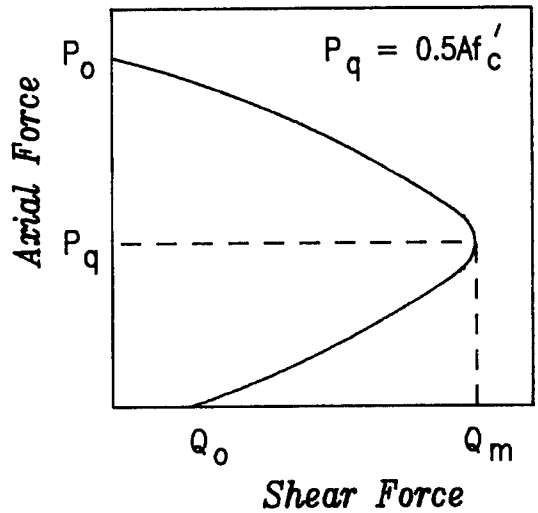

Fig. 10 Relation of Axial Force-Shear Force

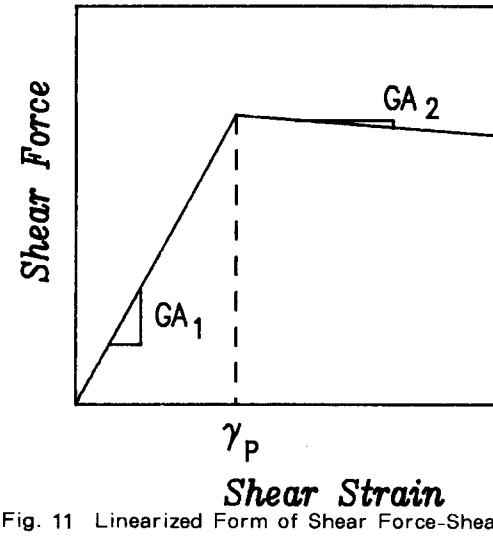

Fig. 11 Linearized Form of Shear Force-Shear Strain

with the test result of frame up to flexural failure[12].

Sectional properties of the under-reinforced beam and element sizes used are shown in Fig. 12. As shown in Fig. 13(a) the results of analyses for these beams are not consistent after peak load when the real moment-curvature curve was used. However, the results using the modified moment-curvature curve are quite consistent as shown in Fig. 13(b). It is shown that the moment-curvature

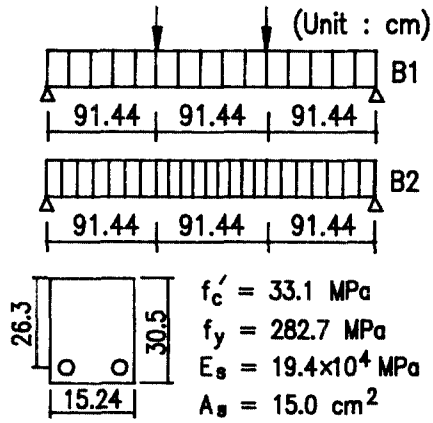

Fig. 12 Sectional Properties and Element Sizes Used

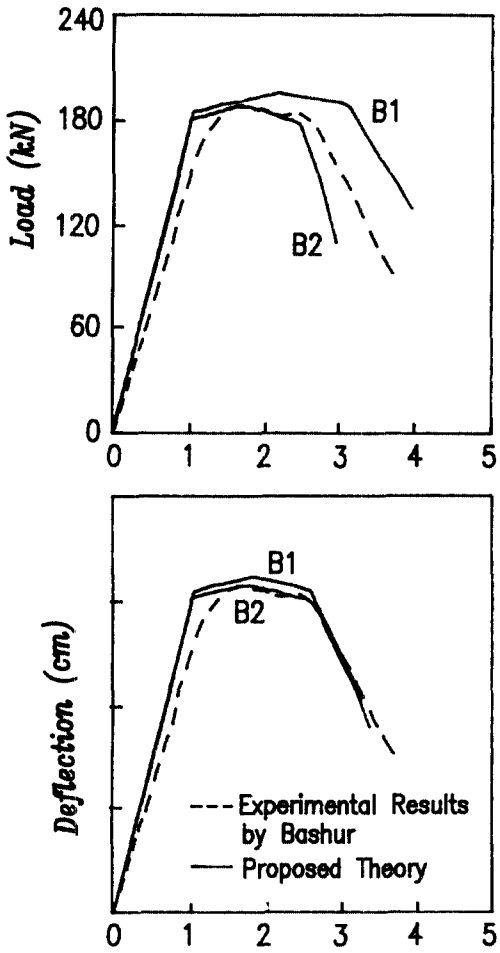

Fig. 13 Load-Deflection Curves for Element Sizes Used

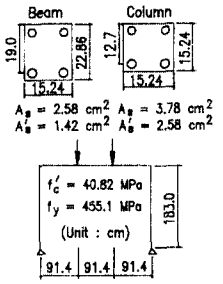

Fig. 14 Sectional Properties and Layout

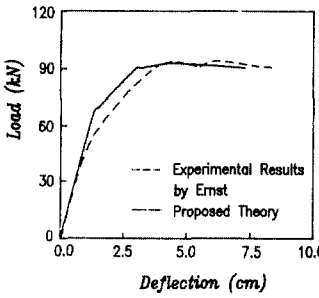

Fig. 15 Load-Deflection Curve Compared with Test Result of Ref. 12

curve has to be modified in order to get consistent result and these results predict well the experimental result by Faud K. Bashur[11].

Fig. 14 shows the sectional properties of the test model and the layout of frame, and the result of the analysis for the frame is shown in Fig. 15. Compared to the test result by George C. Ernst[12], the figure shows that not only load-deflection curve can be completely obtained up to failure, but also the results of analysis by the method suggested in this paper are quite close to the experimental results.

6. CONCLUSIONS

1) Collapse load analysis of reinforced concrete frames has been extended to include a softening stage, using displacement control method. As shown in Figs. 13 and 15, it can be seen that this analytical result predicts well the observed experimental trends.
2) This program provides an more efficient, speedy, and economical method, for a complete analysis of reinforced concrete

frames, than the program by using the layered method.

3) The result of this nonlinear structural analysis considering the strain-softening in finite element method depends on the element size beyond elastic limit. But if the moment-curvature curve is modified for each element by using the concept of fracture energy approach, we can obtain consistent results regardless of the element size adopted.

4) Since the Timoshenko beam theory was applied to present analysis, the obtained peak loads of the load-deflection curve show a little difference as the element size varies.

ACKNOWLEDGEMENT

Financial support under the Asan Foundation to Korea Advanced Institute of Science and Technonogy at 1989 year is greatfully acknowledged.

REFERENCES

1. 김진근, 이태규, 이을범, "변위제어법에 의한 철근콘크리트 보의 비선형 해석", 전산구조공학회지, 제 2 권 제 1 호, pp. 71~78, 1989.

2. A. Fafitis, and S.P. Shah, "Predictions of Ultimate Behavior of Confined Columns Subjected to Large Deformations," J. of ACI, Vol. 82, No, 4, pp. 423~433, 1985.

3. H.N. Arthur, and O.S. Floyd, "Structural Properties of Very High Strength Concrete," Second Progress Report, Cornell University, Ithaca, New York.

4. D.R.J. Owen, and E. Hinton, "Finite Elements in Plasticity : Theory and Practice," Pineridge Press Limited, Swansea, 1980.

5. R. Park, and T. Paulay, "Reinforced Concrete Structures," John Wiley & Sons, New York, 1975.

6. Z.P. Bazant and B.H. Oh, "Crack Band Theory for Fracture of Concrete," Materials and Structures(RILEM, Paris), Vol. 16, pp. 155~177, 1983.

7. W.G. Corley, "Rotational Capacity of Reinforced Concrete Beams," J. of Structural Division, ASCE, Vol. 92, No. ST5, pp. 121~146, 1966.

8. A.H. Mattock, Discussion of "Rotational Capacity of Reinforced Concrete Beams," J. of Structural Division, ASCE, Vol. 93, No. ST2, pp. 519~522, 1967.

9. S.E El-Metwally, and W.F. Chen, "Load-Deformation Relations for Reinforced Concrete Sections," ACI Structural J., Vol. 86, No. 2, 163~167, 1989.

10. Y. Kanoh, K. Minami, K. Takiguchi, and I. Shiraishi, "Shear Mechanism of Reinforced Concrete Members," Proc. of the Seminar sponsored by the Japan Society for the Promotion of Science and the U. S. National Science Foundation, Tokyo, Japan, pp. 308~328, 1985.

11. F.K. Bashur, and D. Darwin, "Nonlinear Model for Reinforced Concrete Slabs," J. of Structural Division, ASCE, Vol. 104, No. ST1, pp. 157~170, 1978.

12. G. C. Ernst, G.M. Smith, and A.R. Riveland, "Basic Reinforced Concrete Frame Performance Under Vertical and Lateral Loads," J. of ACI, Vol. 70, No. 4, pp. 261~269, 1973.